

POSITION MONITORING ON THE ISIS SYNCHROTRON

B. G. Pine, Rutherford Appleton Laboratory, Oxfordshire, UK

Abstract

The ISIS Facility at the Rutherford Appleton Laboratory in the UK produces intense neutron and muon beams for condensed matter research. It is based on a 50 Hz proton synchrotron which, once the commissioning of a new dual harmonic RF system is complete, will accelerate about $3.5E13$ protons per pulse from 70 to 800 MeV, corresponding to mean beam powers of ~ 0.2 MW. Transverse space charge is a key issue for both present and proposed upgrades to the machine, and is the focus of current R&D studies. Experiments on the ISIS ring are central to this work, therefore understanding and quantifying limitations in diagnostics is essential. This paper presents work studying and modelling the ISIS synchrotron beam position monitors.

INTRODUCTION

The ISIS synchrotron has a circumference of 163 m. The vacuum vessels are rectangular and have a varying aperture, averaging half apertures of roughly 80 by 60 mm. Beam is accumulated over 130 turns using charge-exchange injection, and then formed into two bunches during acceleration. Space charge levels are especially high during injection and bunching, though still have a significant effect when the beam is extracted. The ISIS cylindrical split-electrode beam position monitors have operated successfully for many years, but higher intensity operation and related beam studies are motivating a more detailed analysis.

THEORY

Proton bunches in ISIS are relatively long, between 30 and 60 m. With such long bunches, it is assumed that a 2D electrostatic approximation may be used to calculate the position monitor response, as the electromagnetic fields are quasi-steady-state for much of the bunch passage. The purpose of this work was to test whether a 2D approximation was valid, using a simulated 3D monitor. The effects of high frequency bunch passage, and bunch edge effects are likely to also have an effect, but are not considered in this paper.

Laplace's Equation can be solved in 2 dimensions for an off-centre beam in a grounded vacuum vessel [1]. The field can also be calculated using images (*Appendix A*). The surface charge distribution on the inner surface of the grounded vacuum vessel must produce an electric field that cancels this – i.e. is equal to and opposite the beam field at the surface. Therefore the surface charge density can be calculated if the beam field is known. Making the approximation that the electrodes can be treated the same way gives this expression for the total surface charge on one of the electrodes, including the variation of electrode width [2, 3]:

$$Q_1 = -q_b L \int_0^{2\pi} \frac{(1 + \cos\phi)(R^2 - b^2)}{R^2 + b^2 - 2Rb\cos(\phi - \theta)} d\phi \quad (1)$$

where ϕ is the polar angle, R is the electrode radius, b is the radial displacement of the beam and θ is the angular displacement of the beam, q_b is the beam charge density and L is the electrode half length, as in Figure 1.

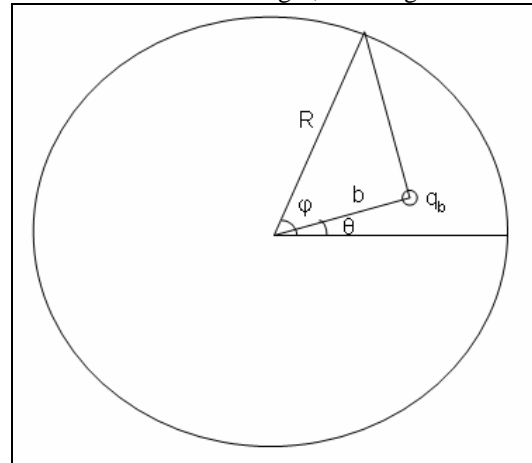


Figure 1: Beampipe geometry.

The solution to this integral is (not obvious, see *Appendix B*):

$$Q_1 = -2\pi q_b L \left(1 + \frac{b}{R} \cos[\theta] \right)$$

And as $x = b\cos[\theta]$,

$$Q_1 = -2\pi q_b L \left(1 + \frac{x}{R} \right)$$

The opposing electrode will have

$$Q_2 = -2\pi q_b L \left(1 - \frac{x}{R} \right)$$

This 2D electrostatic theory predicts that the individual electrode signals will be proportional to the position.

The normalised difference:

$$\frac{Q_1 - Q_2}{Q_1 + Q_2} = \frac{\Delta Q}{\Sigma Q} = \frac{x}{R}. \quad (2)$$

$\frac{\Delta Q}{\Sigma Q}$ is also linear in the displacement, and the gradient of the difference-over-sum (DoS) curve is equal to $1/R$.

SIMULATIONS

ISIS split-cylinder capacitive position monitors have been modelled with CST Studio Suite [4], and the results compared with the theory discussed above.

Most of the ISIS monitors are centred around the beampipe, and have a rectangular vacuum vessel which cuts into their housing, as can be seen in Figure 2.

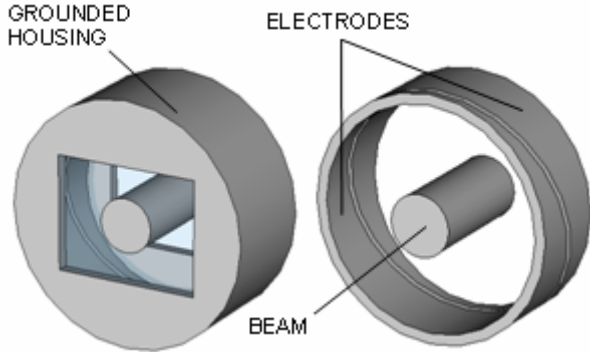


Figure 2: ISIS position monitor.

There are other designs, for instance in the extraction straight there are larger monitors, which allow for the vertical displacement of the beam during extraction, and measure in both planes; one of these designs is shown in Figure 3.

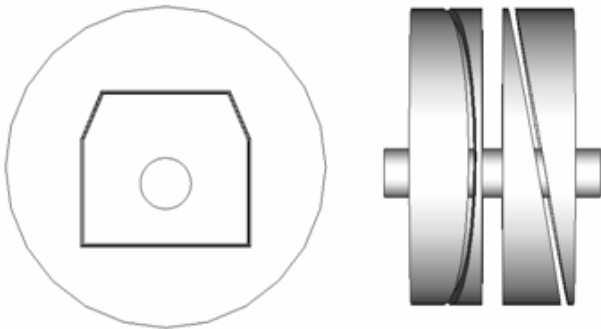


Figure 3: ISIS synchrotron Straight 1 position monitor.

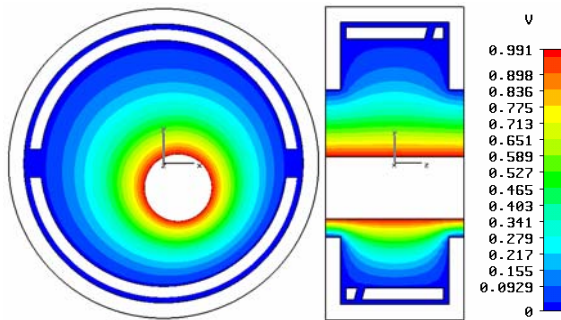


Figure 4: ISIS position monitor potentials with offset beam: surface beam potential normalised to 1V in this case.

These models were created using perfect conductors to form the vacuum vessel and electrodes. The beam was made from perfect conductor with a constant potential on the surface in early models, and later a volume of constant charge density replaced this. The vacuum vessels were fixed at 0 V, and the electrodes given a “floating” potential which allowed them to vary to fit the environment. Electrode potentials calculated by the CST Electrostatic Solver were recorded as the beam was moved around the transverse plane. Electric boundary

conditions were used around the vacuum vessel, and magnetic at the open end ends of the beampipe. The potential distribution for an offset beam with one of the standard monitors is shown in Figure 4.

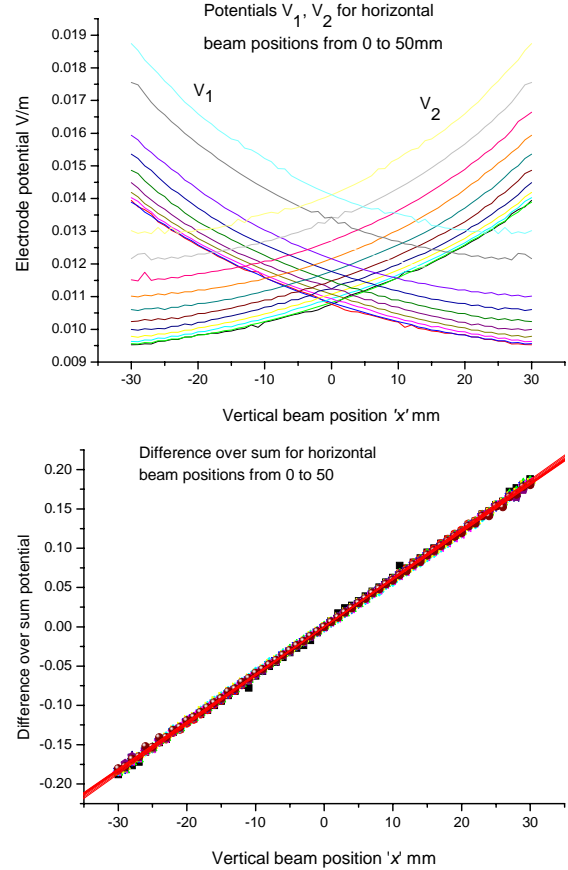


Figure 5: (a) Electrode potentials and (b) Difference over sum for a vertical monitor.

A set of results obtained from the CST model determined the electrode potential as the beam was scanned over both transverse dimensions. Figure 5(a) shows the electrode potentials V_1 and V_2 , and Figure 5(b) shows the DoS for those potentials.

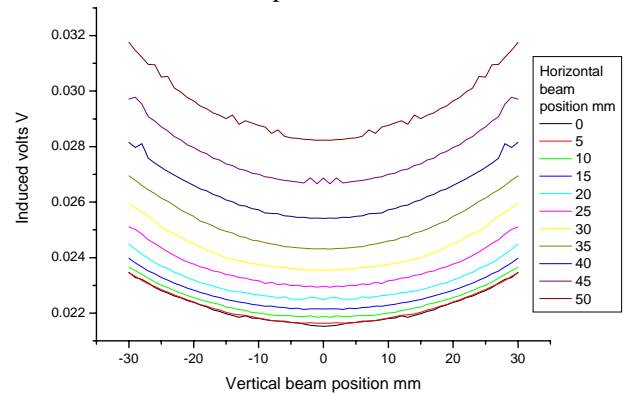


Figure 6: Electrode sum signal for beam position varying in both horizontal and vertical planes.

As can be seen, the DoS is linear across the whole aperture of the monitor, though the individual electrode signals are not linear. It was found that the value of the

DoS gradient deviated significantly from $1/R$. The 2D theory assumes that the total charge induced on the electrodes (the sum signal) is constant, whereas the simulations show that the sum potential of the two electrodes also varies with beam position, Figure 6.

Another feature was explored by taking one of the standard synchrotron monitor models, and stretching the longitudinal dimension of the monitor. As the monitor was stretched, its behaviour grew asymptotically closer to the simple theory – the inverse constant of proportionality tended to the electrode radius. If a position monitor were created infinitely long it would act the same way as the 2D theory predicts, see Figure 7.

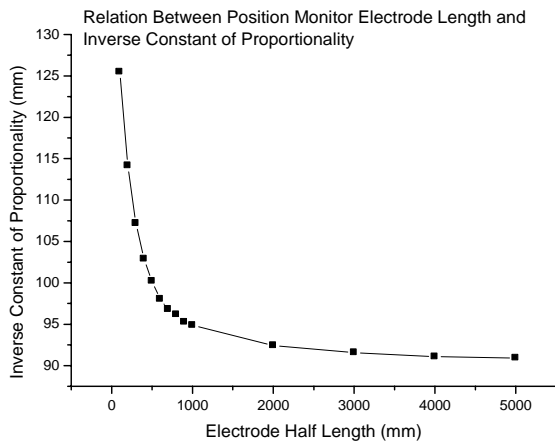


Figure 7: Inverse DoS gradient (R) versus electrode half-length for a model with electrode radius = 90 mm.

BEYOND 2D

Simple 2D theory describes some of the features that the simulations display, such as DoS linearity, but not others. Is there some way of extending the simple theory so that it is sufficient to describe the monitor fully without resorting to simulation? In 1977, J. H. Cuperus wrote a paper 'Edge Effect in Beam Monitors' [5], in which the non-linearities contributed by transitions in the beam pipe are studied. He concluded that additional grounded electrodes should be added at the front and back of the monitor. If these guard electrodes are sufficiently long then they counter the effect of a transition near the monitor, and 2D theory is sufficient to describe the beam behaviour, examples can be seen in Figure 8.

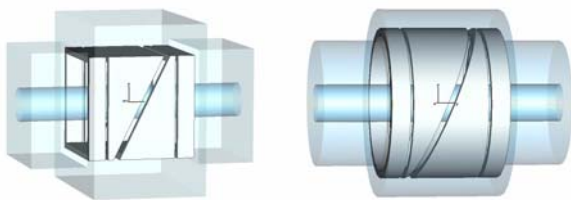


Figure 8: Monitors with guard electrodes.

His paper uses a form of perturbation theory, to iterate through improvements for a guessed shape of perturbed potential at the beam pipe transition. He discovered that the answers came in an infinite series, but that most

elements in the series could be discarded if the guard electrodes were sufficiently long.

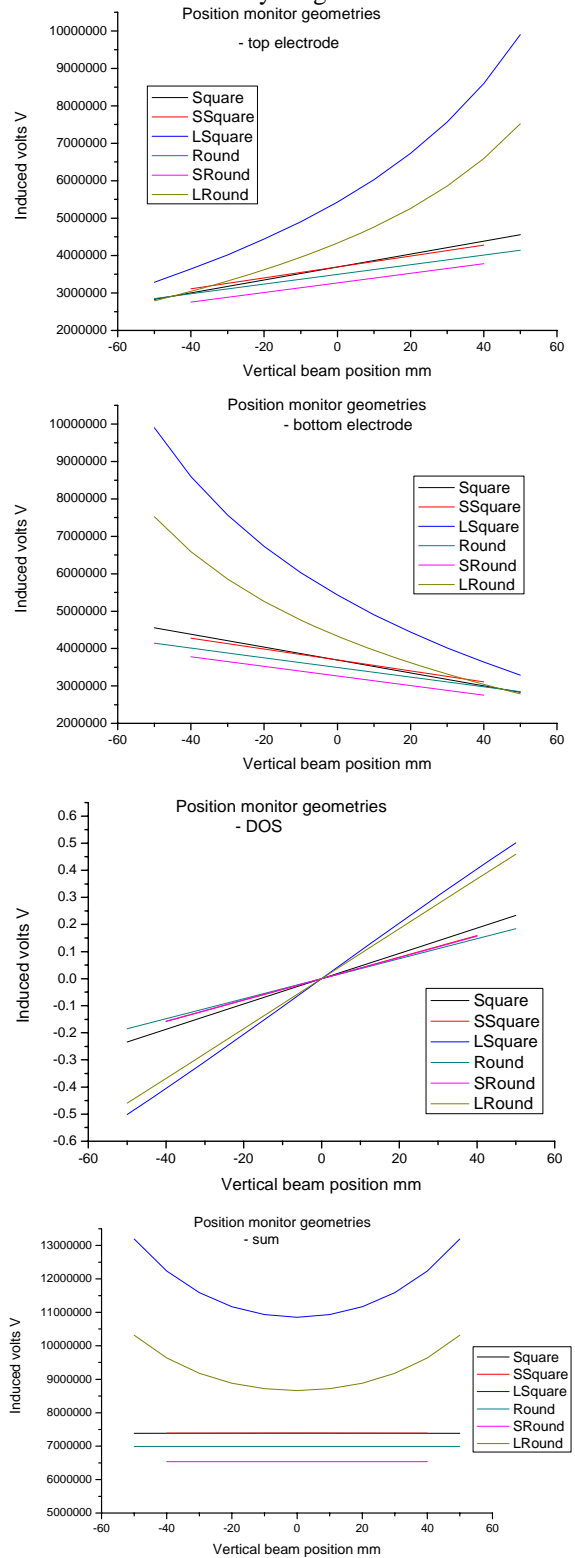


Figure 9: Effect of guard electrodes: Square and Round have electrodes the same size as the beam pipe, which are square and round in shape respectively; SSquare and SRound have electrodes smaller than the beam pipe; LSquare and LRound have electrodes larger than the beam pipe.

Figure 9 shows the simulated response of a set of monitors with guard electrodes. There are 6 variations: square monitor in square beampipe with electrodes bigger, equal and smaller than the beampipe; and the same for a round monitor in a round beampipe. As can be seen, the electrode responses are linear for both shapes if the electrodes are smaller than or equal to the size of the beampipe. Further work could be done here, as it seems possible that longer guard electrodes would make even the larger monitors linear.

ISIS monitors do not have guard electrodes, and it would be troublesome to install them now. There are also difficulties repeating Cuperus's calculation: ISIS monitors have a rectangular beampipe going into a larger cylinder housing the cylindrical electrodes, which makes the geometry more complex. As there is no guard, higher order elements in the infinite series solution must be considered, and this makes the perturbations very difficult to calculate. Still this is an interesting area for further study.

CONCLUSION

It has become clear that 2D theory is not sufficient to account for the behaviour of the ISIS synchrotron position monitors. While the behaviour of the difference over sum output may well still be linear, the gradient of this line is different from that predicted by theory.

It is apparent that this difference is primarily due to transitions in the beampipe shape and size near to the electrodes, and could be factored out by including sufficiently long guard electrodes in the monitor design. As this would be difficult to achieve for the current monitors, a possible correction is being considered using theory, simulations and experimental verification.

However, monitors built in the future for ISIS or ISIS upgrades would certainly be planned with guard electrodes from the beginning.

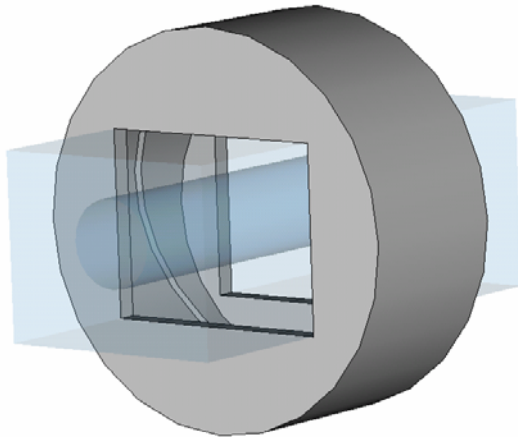


Figure 10: Monitor simulated with beampipe.

FUTURE WORK

At time of writing the iteration cycle that Cuperus used has been recreated, but there is still a great deal of uncertainty about applying the method to the ISIS

monitors. Simultaneously then, another set of simulations are running in CST, to take more account of the beampipe environment near the monitors, see Figure 10.

Work studying the effects of high frequency bunch passage through the monitors is also anticipated, both using CST Microwave Studio, and with further analysis.

REFERENCES

- [1] E. Regenstreif, "Electrostatic beam potential created by a uniform round beam coasting off centre in a circular vacuum chamber", CERN Report, 1976.
- [2] R. E. Shafer, "Beam Position Monitoring", AIP Conference Proceedings Vol 212, (1989).
- [3] A. Hofmann, CAS 1992 Proceedings, CERN 94-01, p342 (1994).
- [4] www.cst.com.
- [5] J. H. Cuperus, "Edge Effect in Beam Monitors", Nuclear Instruments and Methods 145 (1977) 233-243.
- [6] C. R. Prior, private correspondence.

APPENDIX A: IMAGE METHOD

The electric field parallel to the beam pipe boundary must be zero, and the electric field perpendicular to it must be proportional to the surface charge. Assume there is another line charge with the opposite charge to the beam, situated outside the cylinder, a distance l from the axis, see Figure 11.

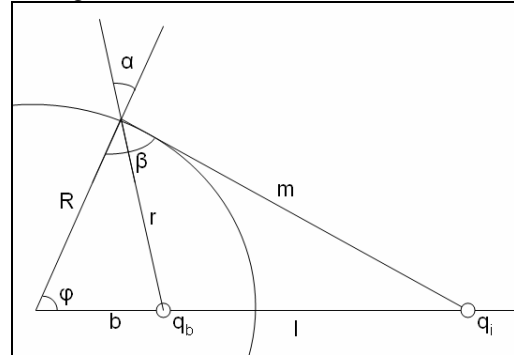


Figure 11: Beampipe geometry with images.

We try to satisfy the boundary condition on the surface such that $E_{||} = E_{\phi} = 0$.

The beam field:

$$E_{\phi b} = \frac{\lambda}{2\pi\epsilon_0} \frac{1}{r} \text{Sin}\alpha$$

And the image field:

$$\begin{aligned} E_{\phi i} &= -\frac{\lambda}{2\pi\epsilon_0} \frac{1}{m} \text{Cos}(\beta - 90) \\ &= -\frac{\lambda}{2\pi\epsilon_0} \frac{1}{m} \text{Sin}\beta \end{aligned}$$

Beam and image fields parallel to boundary cancel:

$$E_{\phi b} + E_{\phi i} = 0 = \frac{\lambda}{2\pi\epsilon_0} \frac{1}{r} \text{Sin}\alpha - \frac{\lambda}{2\pi\epsilon_0} \frac{1}{m} \text{Sin}\beta$$

$$\begin{aligned}
&= \frac{\lambda}{2\pi\epsilon_0} \left(\frac{1}{r} \frac{b \sin\phi}{r} - \frac{1}{m} \frac{l \sin\phi}{m} \right) \\
b(R^2 + l^2 - 2Rl \cos\phi) &= l(R^2 + b^2 - 2Rb \cos\phi) \\
&= bl^2 - (R^2 + b^2)l + bR^2
\end{aligned}$$

Solving this last equation leads to either $l = b$ or $l = \frac{R^2}{b}$.

Then using this result, we find the field perpendicular to the vacuum vessel:

$$\begin{aligned}
E_{\rho b} + E_{\rho i} &= \frac{\lambda}{2\pi\epsilon_0} \frac{1}{r} \cos\alpha - \frac{\lambda}{2\pi\epsilon_0} \frac{1}{m} \cos\beta \\
&= \frac{\lambda}{2\pi\epsilon_0} \left(\frac{1}{r} \frac{R^2 + r^2 - b^2}{2Rr} - \frac{1}{m} \frac{R^2 + r^2 - l^2}{2Rm} \right) \\
&= \frac{\lambda}{4\pi\epsilon_0 R} \left(\frac{R^2 - b^2}{r^2} - \frac{R^2 - l^2}{m^2} \right) \\
&= \frac{\lambda}{4\pi\epsilon_0 R} \left(\frac{2R^2 - 2b^2}{R^2 + b^2 - 2Rb \cos\phi} \right)
\end{aligned}$$

Which is equal to the surface charge distribution on the inside of the cylinder. This equation for the total surface charge is called the Poisson Integral:

$$Q = \frac{\lambda}{2\pi\epsilon_0 R} \int_0^{2\pi} \frac{R^2 - b^2}{R^2 + b^2 - 2Rb \cos\phi} d\phi$$

APPENDIX B: SOLUTION TO EQUATION [1]

Equation (1) combines the Poisson equation with the electrode width and can be solved using complex analysis. Many thanks to C. R. Prior for the solution [6].

$$Q = -q_b L \int_0^{2\pi} \frac{(1 + \cos\phi)(R^2 - b^2)}{R^2 + b^2 - 2Rb \cos(\phi - \theta)} d\phi$$

Let $\bar{R} = R e^{i\phi}$ and $\bar{b} = b e^{i\theta}$,

then $\bar{R}\bar{R}^* = R^2$, $\cos\phi = \frac{\bar{R} + \bar{R}^*}{2R}$,

$$R^2 + b^2 - 2Rb \cos(\phi - \theta) = |\bar{R} - \bar{b}| |\bar{R}^* - \bar{b}^*|,$$

and $d\bar{R} = i R e^{i\phi} d\phi = i \bar{R} d\phi$

$$\begin{aligned}
Q &= -q_b L (R^2 - b^2) \oint \frac{\left(1 + \frac{\bar{R} + \bar{R}^*}{2R}\right) d\bar{R}}{|\bar{R} - \bar{b}| |\bar{R}^* - \bar{b}^*| i \bar{R}} \\
&= -\frac{q_b L (R^2 - b^2)}{2R} \oint \frac{\left(2R + \bar{R} + \frac{R^2}{\bar{R}}\right) d\bar{R}}{|\bar{R} - \bar{b}| \left| \frac{R^2}{\bar{R}} - \bar{b}^* \right| i \bar{R}} \\
&= -\frac{q_b L (R^2 - b^2)}{i2R} \oint \frac{(2R\bar{R} + \bar{R}^2 + R^2) d\bar{R}}{\bar{R} |\bar{R} - \bar{b}| |R^2 - \bar{b}^* \bar{R}|}
\end{aligned}$$

This equation has poles at $\bar{R} = 0$, $\bar{R} = \bar{b}$ and $\bar{R} = \frac{R^2}{\bar{b}}$, but only the first two are correct as $\frac{R^2}{\bar{b}}$ is always greater than R , for $b < R$.

Residue for $\bar{R} = 0$,

$$R[0] = \frac{q_b L (R^2 - b^2)}{i2R} \frac{R^2}{\bar{b} R^2} = \frac{q_b L (R^2 - b^2)}{i2R \bar{b}}$$

Residue for $\bar{R} = \bar{b}$,

$$\begin{aligned}
R[\bar{b}] &= -\frac{q_b L (R^2 - b^2)}{i2R} \frac{(2R\bar{b} + \bar{b}^2 + R^2)}{\bar{b} |R^2 - \bar{b}^* \bar{b}|} \\
&= -\frac{q_b L (R^2 - b^2)}{i2R} \frac{(2R\bar{b} + \bar{b}^2 + R^2)}{\bar{b} (R^2 - b^2)}
\end{aligned}$$

$Q = 2\pi i \times \text{Sum of residues}$

$$\begin{aligned}
&= 2\pi i \times \frac{q_b L (R^2 - b^2)}{i2R} \left[\frac{1}{\bar{b}} - \frac{(2R\bar{b} + \bar{b}^2 + R^2)}{\bar{b} (R^2 - b^2)} \right] \\
&= -\frac{\pi q_b L}{R} \left[\frac{b^2}{\bar{b}} + \bar{b} + 2R \right] \\
&= -\frac{\pi q_b L}{R} [2R + \bar{b} + \bar{b}^*] \\
&= -2\pi q_b L \left[1 + \frac{b}{R} \cos\theta \right]
\end{aligned}$$